Design of Localizer Capture and Track Modes for a Lateral Autopilot Using *H*-Infinity Synthesis

Isaac Kaminer, Pramod P. Khargonekar, and Greg Robel

ABSTRACT: This paper presents the results of a design exercise in which the most recent developments in *H*-infinity synthesis theory were applied to the problem of designing a lateral autopilot for a typical transport airplane. The bulk of the engineering effort in applying these results was in the formulation of an appropriate synthesis model. We present some of the important aspects of this process. The linear controller design was done using *H*-infinity synthesis theory. The linear design was suitably modified to satisfy some of the performance constraints. Results of linear analysis and simulation of the final nonlinear controllers are presented.

Introduction

The objective of the design exercise was to apply the recently developed state-space algorithms for *H*-infinity control synthesis [2, 4–6, 9] to this problem. The problem statement requires the design of two lateral autopilot modes: heading hold and localizer capture and track. In the heading hold mode, the autopilot is to provide independent control of heading and sideslip angles; in the localizer capture and track mode, the autopilot is to control localizer beam deviation and sideslip angle to zero.

The key steps in our synthesis procedure were as follows. A nominal design point was first selected. Then we converted the given performance and robustness specifications into a standard *H*-infinity synthesis problem. This is, of course, the most interesting and difficult step. The important features of this step are described in the section on the feedback regulator design; however, that description is by no means complete. This was followed by a routine application of the *H*-infinity synthesis procedure which led to the nominal linear design. This design was then gain scheduled to operate over the given flight envelope. Finally, modifications were made to take into account the limits on various physical variables, thus resulting in the final nonlinear design.

This article is organized as follows. First, we present the problem statement and the performance and stability requirements to be satisfied. Then we briefly describe the physics of the problem, i.e., the airplane's equations of motion, derivation of linearized models, etc., followed by the presentation of the highlights of our design exercise. Next, the results of our analysis of the performance and robustness characteristics of the controller are discussed. The article ends with some conclusions.

Problem Statement

It is desired to design an autopilot to control the lateral axis of transport airplane. The autopilot is required to control heading to establish and maintain a pilot heading command. In addition the autopilot should be able to latch onto an Instrument Landing System (ILS) localizer beam and control the airplane to fly along the beam as it makes an approach to land. At all times the autopilot should regulate sideslip angle (β) around zero to provide turn coordination.

The performance requirements are as follows. There should be zero steady state error: the heading error should be zero when in heading mode; the localizer crosstrack error should be zero when following the ILS localizer beam; and the crosswind should not cause steady state errors in either mode. There should be zero time domain overshoot: the heading overshoot should be zero when in heading mode; the localizer beam overshoot should be zero when following ILS localizer beam (assuming capture is initialized with sufficient space to turn onto the beam without crossing the center line); and the steady crosswind should not cause overshoot in either mode. There are response limitations: the bank angle should not exceed 30° during maneuvers; the lateral acceleration (nominally zero) should not exceed 0.05 g for maneuvers in still air; and the airplane should not bank into the beam if the initial crosstrack angle (at the beginning of the capture) exceeds 30°. There are bandwidth requirements: maximize response bandwidths within limitations on overshoot, surface activity, eigenvalues, and disturbance responses. There are control activity requirements: the aileron activity is limited because position should not exceed ±15°, and rate should not exceed ±30°/s; the rudder activity is limited because position should not exceed ±15°, and rate should not exceed ±30°/s. There are robustness requirements: the eigenvalue requirements are that all eigenvalues should have a damping of 0.4 or better, and dominant eigenvalues should have a damping of 0.6 or better; stability margins; aileron input requirements are simultaneous ±4 dB and ±40°; rudder input requirements are simultaneous ±4 dB and ±40°; and all sensor input requirements are simultaneous ±4 dB and ±40°.

Feedback Regulator Design

In this section, we will describe the key features of the controller design process which we followed. The section is organized into a number of subsections that emphasize some of the important engineering issues that arose in the controller design. The localizer capture and track controller was designed first. The heading hold controller was then obtained by nulling appropriate gains in the localizer controller.

Airplane Model Description

The design problem to be solved in this paper deals with the lateral directional motion of the airplane and the control of the lateral rigid body dynamics. A complete description of the airplane's equations of motion can be found in many available references. One such reference is [11]. Con-

Presented at the 1989 American Control Conference, Pittsburgh, PA, June 21-23, 1989. I. Kaminer was with the Guidance and Control Research Group of the Boeing Company, Seattle, WA 98124. He is now with the Department of Electrical Engineering and Computer Science, University of Michigan, Ann Arbor, MI 48109. P. P. Khargonekar is with the Department of Electrical Engineering and Computer Science, University of Michigan, Ann Arbor, MI 48109. G. Robel is with Guidance and Control Research, Boeing Commercial Airplanes, Seattle, WA 98124.

0272-1708/90/0600-0013 $01.00 © 1990 IEEE

sequently, we will not describe the equations of motion in detail. Rather we will present a brief qualitative description of the key features of the airplane dynamics.

The lateral directional equations of motion of the airplane are described by one force equation (lateral force Y) and two angular moment equations (rolling moment L and yawing moment N). The state variable associated with the Y equation is the sideslip angle β, and the state variables associated with the rolling and yawing moments, L and N, are roll rate P and yaw rate R, respectively. The Euler angles corresponding to the angular rates are the heading angle Ψ (the angle between the body fixed x-direction of the airplane's motion and North) and the bank angle ϕ (the angle between the horizon and the wings of the airplane). Other motion variables of interest are groundtrack heading Ψ_{gt} (the angle between the inertial x-direction of the airplane's motion and North) and β_{air} (the sideslip angle in the wind-relative coordinate system). The importance of the two latter variables will become clear in the section on the effects of the crosswind. Fig. 1 illustrates the definitions of the aforementioned variables. All the angles used in this paper are expressed in degrees, angle rates in °/s, position variables in feet, position rates in ft/s, and accelerations in ft/s^2.

The linear models used in this paper are a set of small perturbation equations linearized at 14 operating points. At each point all the angles and rates were set to 0. Further details on the operating points are given in the section on the nominal model selection.

The linear model of the lateral airplane consists of four states: β, P, ϕ, R; and two control effectors: δ_a (aileron deflection) and δ_r (rudder deflection). Two states must be added to enable one to design the heading and localizer modes (described below): Ψ (airplane's heading) and y (lateral displacement). They are defined as:

$$\Psi = (1/s)R \tag{1}$$

$$y = (1/s)V_i \sin \Psi \tag{2}$$

where V_i is the inertial speed of the airplane. For the given operating conditions perturbations in ϕ and Ψ can be shown to be direct integrals of P and R.

The lateral directional rigid body motion of the airplane is characterized by the second order dutch roll mode (stable, but highly underdamped) and the first order roll and spiral modes (both stable and real). Closing the ϕ and Ψ loops, which is necessary for the problem considered here, creates a second order heading mode. The motions involve perturbations in β, R, P, ϕ, and Ψ. For the type of the aircraft considered in the paper the frequencies are of the order of 2 rad/s for the dutch roll and roll modes and 0.01 rad/s for the spiral mode. The desired frequency for the heading mode depends on the application and is discussed in the section on the feedback regulator design. The primary control effector for the dutch roll and spiral modes is rudder, located on the vertical tail of the airplane, and for the roll and heading modes are ailerons, located on the wings.

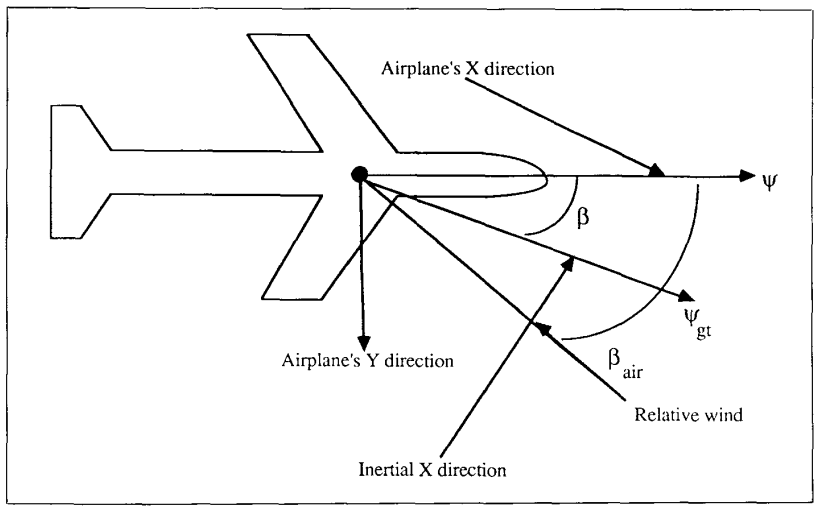

Fig. 1. Basic airplane definitions.

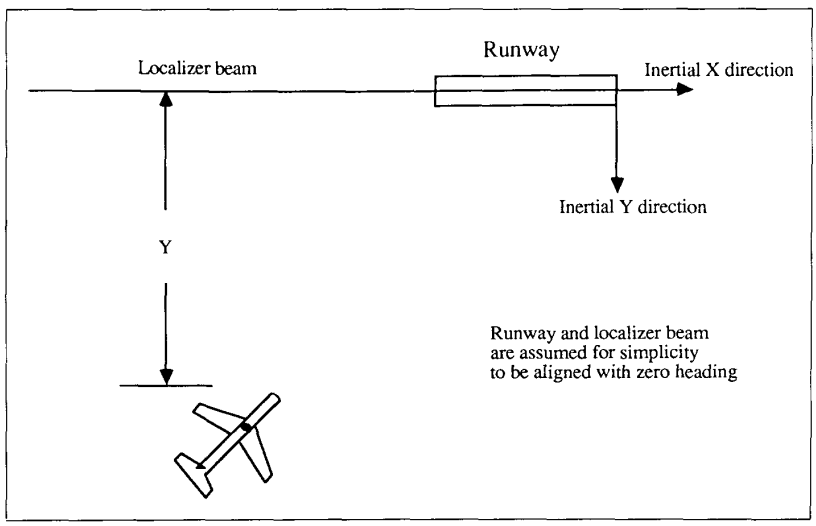

Fig. 2. Localizer geometry.

The geometry for the localizer capture and track problem to be solved here is shown in Fig. 2. Initially the airplane is several thousand feet away from the localizer beam, which points to the center of the runway. The airplane must establish a nonzero cross-track angle (the angle between the airplane's inertial x-direction and the runway heading) and maintain it until an overshoot free capture of the localizer beam can be accomplished, at which point the controller is to initialize the capture and align the airplane with the runway centerline and track the localizer beam to touch down. The airplane is assumed to be initially far enough from the beam to allow an overshoot free capture. This maneuver requires the design of the heading mode to maintain nonzero cross-track angle and of the localizer capture and track mode.

On a typical commercial airplane, all the lateral state variables, except β, are available for feedback. Moreover, β can be computed

using the available signals. Therefore, a decision was made to design a state-feedback control law for reasons of simplicity. Issues of implementation will be discussed later in the paper.

Nominal Design Point

A total of 14 flight conditions were given for which the design requirements were to be satisfied. They were obtained by linearizing the equations of motion at the typical landing conditions: altitude of 100 ft above sea level, total of seven flap settings from 0 to 35°. (Flaps are high lift devices on the leading and trailing edges of the wings used to improve airplane's lift characteristics for low speed manuevers such as take off and landing). At each flap setting the airplane was linearized at the minimum and maximum allowable speeds. After a review of all the given flight conditions, we chose the flight condition with flaps set at 25° and inertial speed of 321 ft/s as the nominal design point. The inertial speed of 321 ft/s corresponds to a maximum allowable speed for this flap setting.

H-Infinity Synthesis

Consider the feedback system shown in Fig. 3. Let T_{zw} denote the closed-loop transfer matrix from the input vector w of exogenous signals, to the output vector z of errors to be reduced. The H-infinity synthesis problem is to find, among all controllers that yield a stable closed-loop system, a controller K that minimizes the infinity norm of T_{zw}. (The infinity norm of a stable transfer matrix is the maximum over all frequencies of its largest singular value, and may be interpreted as its maximum energy gain.) Recent work [2, 4-6, 9] has led to a simple and elegant approach to this problem. We will confine our attention here to the state feedback case [2, 5, 9].

Suppose that a state-space realization for the plant depicted in Fig. 3 can be written as

$$\dot{x} = Ax + B_1 w + B_2 u$$

$$z = C_1 x + D_{12} u$$

$$y = x.$$

Assume that (A, B_2) is stabilizable, and that D_{12} has linearly independent columns. Recall that a Hamiltonian matrix is a matrix H of the following form where A, Q, and R are real $n \times n$ matrices with Q and R symmetric:

$$H = \begin{bmatrix} A & R \\ Q & -A^T \end{bmatrix}.$$

If such a matrix H has no imaginary eigenvalues, then the spectral subspace $\chi_-(H)$ spanned by the generalized eigenvectors belonging to eigenvalues lying in the open left half-plane is of dimension n. Let X_1 and X_2 denote a basis for the subspace $\chi_-(H)$. We will say that the Hamiltonian matrix H belongs to *dom*(Ric) if H has no imaginary eigenvalues, and if X_1 is nonsingular. If H belongs to *dom*(Ric), define $\mathrm{Ric}(H) := X_2 X_1^{-1} =: X$. It is well known that X is symmetric, $P + RX$ is stable, and X satisfies the algebraic Riccati equation

$$P^T X + XP + XRX - Q = 0.$$

The key mathematical result on H-infinity synthesis used in this paper is stated below.

Theorem: Suppose $\gamma > 0$ is a given positive number. Let

$$H(\gamma) = \begin{bmatrix} H_{11} & H_{12} \\ H_{21} & H_{22} \end{bmatrix}$$

where

$$H_{11} = A - B_2(D_{12}^T D_{12})^{-1} D_{12}^T C_1$$

$$H_{12} = \gamma^{-2} B_1 B_1^T - B_2(D_{12}^T D_{12})^{-1} B_2^T$$

$$H_{21} = -C_1^T(I - D_{12}(D_{12}^T D_{12})^{-1} D_{12}^T) C_1$$

$$H_{22} = -A^T + C_1^T D_{12}(D_{12}^T D_{12})^{-1} B_2^T.$$

Then there exists a stabilizing controller K such that $\|T_{zw}\|_\infty < \gamma$ if and only if $H(\gamma) \in$ *dom*(Ric) and $X(\gamma) := \mathrm{Ric}(H(\gamma))$ is positive definite. In this case, one such controller is $K(s) = F$, where

$$F = -(D_{12}^T D_{12})^{-1} [D_{12}^T C_1 + B_2^T X(\gamma)].$$

Testing whether $H(\gamma) \in$ *dom*(Ric), and solving for $X(\gamma)$ in case it is, can be accomplished using a standard technique [7] for solving Riccati equations, based on the real Schur decomposition.

This theorem is used in the following ways. First, a stabilizing state feedback gain matrix K is computed, using the aforementioned formulas with $\gamma = \infty$. (This step yields an optimal LQR gain.) The infinity norm of the resulting closed-loop transfer matrix T_{zw} is then computed, using the algorithm in [10]. This gives an upper bound γ_u on the achievable performance. The theorem is then used to perform a binary search in the interval $[0, \gamma_u]$ for the optimal value of γ. Once the binary search has determined a sufficiently small interval in which the optimal value of γ must lie, the search is terminated, and a (nearly optimal) state feedback gain matrix is computed using the right-hand endpoint of this interval for γ in the formulas above.

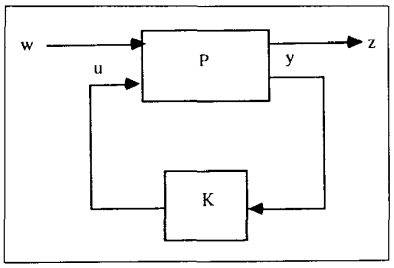

Fig. 3. Standard feedback configuration.

Plant Uncertainty and Formulation of the Synthesis Model

The H-infinity problem as formulated above does not explicitly address the issue of plant uncertainty. But if one models the plant uncertainty as an unknown but norm-bounded, stable dynamical system, and if one includes the inputs and outputs of the plant uncertainty block in z and w, respectively, then H-infinity optimization can provide robustness against plant uncertainty [1, 3]. If this is done, then the vectors z and w have the form shown where the vector w_{perf} consists of the exogenous signals (commands and disturbances), the vector z_{perf} consists of the errors to be reduced, and vectors z_{un} and w_{un} are the input and output to the plant uncertainty block, respectively:

$$z = \begin{bmatrix} z_{\mathrm{perf}} \\ z_{\mathrm{un}} \end{bmatrix}$$

$$w = \begin{bmatrix} w_{\mathrm{perf}} \\ w_{\mathrm{un}} \end{bmatrix}.$$

Next, the formulation of the performance vectors w_{perf} and z_{perf} is discussed, followed by a discussion of uncertainty modeling and of the uncertainty inputs and outputs z_{un} and w_{un}.

The choice of w_{perf} and z_{perf} was based on the performance requirements. For the design problem considered here, zero steady-state error is required for the sideslip and localizer deviation errors (β_e and y_e); hence, two error outputs were created. Let β_c denote the sideslip command and y_c denote the lateral position command with respect to the beam. Then

$$\beta_e = \beta_c - \beta \tag{4}$$

$$y_e = y_c - y. \tag{5}$$

Integrators were placed on each error output. Also, the control inputs must be a part of z_{perf} for the synthesis problem to be well defined. Therefore, the initial choices for z_{perf} and w_{perf} were: $[(1/s)\beta_e \ (1/s)y_e \delta_a \delta_r]^T$ and

$[y_c \beta_c]^T$, respectively. The weighting selection for each entry in z_{perf} was based on the bandwidth requirements. Thus, the weightings on the integrated error outputs were adjusted to achieve the desired command response bandwidth of 1 rad/s in the β/β_c loop and 0.12 rad/s in the y/y_c loop. The weightings for aileron and rudder outputs were modified to achieve a 3 rad/s crossover in the rudder loop and 1 rad/s crossover in the aileron loop. The weighting selection for the outputs (integrated errors in this case) was done using the following property of the solution: an increase in the integrator weighting results in the increase of the corresponding command loop bandwidth and vice versa. The weighting selection for the control inputs (included in z_{perf} vector) follows the opposite pattern, i.e., an increase in the weighting results in the decrease of the corresponding control bandwidth and vice versa. For example, increasing the weighting on δ_r entry will decrease the rudder control bandwidth and increasing the weighting on $(1/s)y_e$ will increase the bandwidth in y/y_c loop.

After several iterations the desired crossovers in command and control loops were achieved. But the dutch roll damping ratio remained low, around 0.25, which is considerably below the closed-loop damping requirement. To improve the dutch roll damping, the states ψ and β were added to z_{perf}. This change improved the damping only slightly. But the addition of the $\dot{\beta}$ output to z_{perf} resulted in the dramatic improvement of the damping ratio after only a few adjustments of the weighting on $\dot{\beta}$. The explanation for the improvement is that the dutch roll motion is most pronounced in the $\dot{\beta}$ output. This can be seen from the frequency response of $\dot{\beta}/\beta_c$ transfer function. In fact, the peak in the $\dot{\beta}/\beta_c$ response (its infinity norm) occurs at the dutch roll frequency. In general, the desired damping for the given mode using H-infinity synthesis can usually be achieved by including in z_{perf} an output which attains its infinity norm at the frequency of the mode to be damped. Then, by adjusting the weighting on the output, most likely increasing it, the desired damping can be achieved. Why should this be true? The H-infinity solution tends to flatten out the T_{zw} frequency response (see Fig. 3). Therefore. by including the kind of output described above in the z vector and putting a large penalty on it will make the peak due to the underdamped mode very evident in the T_{zw} response. Then the H-infinity solution will flatten out the peak, thus improving the damping of the particular mode. The resulting z_{perf} vector is shown in (6):

$$z_{perf}^T = \left[0.2 \int \beta,\ 0.03 \int y_e,\ 10\psi,\ 300\beta,\ 30\dot{\beta},\ 10\delta_a,\ 50\delta_r\right]. \tag{6}$$

The exogenous input vector w_{perf} consisted of β_c, ψ_R, and y_c (sideslip command, runway heading angle, and lateral displacement command, respectively). The variable ψ_R is necessary to compute the airplane's lateral displacement with respect to the runway centerline:

$$y = (1/s) V_i \sin(\psi - \psi_R). \tag{7}$$

The uncertainty modeling for this problem was done along the lines of [3]. The major uncertainties occur in the aerodynamic coefficients, which represent incremental forces and moments generated by incremental changes in sideslip, aileron, and rudder angles (δ_β, δ_a, δ_r) as shown:

$$\begin{bmatrix} y \\ n \\ l \end{bmatrix} = \begin{bmatrix} c_{y\beta} & c_{ya} & c_{yr} \\ c_{n\beta} & c_{na} & c_{nr} \\ c_{l\beta} & c_{la} & c_{lr} \end{bmatrix} \begin{bmatrix} \delta_\beta \\ \delta_a \\ \delta_r \end{bmatrix} \tag{8}$$

where

y, n, l	incremental lateral force, rolling, and yawing moments,
$c_{y\beta}$, $c_{n\beta}$, $c_{l\beta}$	incremental force and moments due to δ_β,
c_{ya}, c_{na}, c_{la}	incremental force and moments due to δ_a, and
c_{yr}, c_{nr}, c_{lr}	incremental force and moments due to δ_r.

Each coefficient in (8) is represented as a sum of a nominal value plus a perturbation:

$$c = c_0 + \delta.$$

The uncertainty source was modeled to be the same for each column in (8):

$$\begin{bmatrix} y + \delta y \\ n + \delta n \\ l + \delta n \end{bmatrix} = \begin{bmatrix} c_{y\beta} + \delta_1 & c_{ya} + \delta_2 & c_{yr} + \delta_3 \\ c_{n\beta} + \delta_1 & c_{na} + \delta_2 & c_{nr} + \delta_3 \\ c_{l\beta} + \delta_1 & c_{la} + \delta_2 & c_{lr} + \delta_3 \end{bmatrix} \cdot \begin{bmatrix} \delta_\beta \\ \delta_a \\ \delta_r \end{bmatrix}. \tag{9}$$

The 14 flight conditions given for this problem were used to establish bounds on each δ_i. The norm of the maximum variation of each column over all flight conditions was used as a (conservative) bound on the respective δ_i:

$$|\delta_1| < 5$$
$$|\delta_2| < 1.5$$
$$|\delta_3| < 2.$$

The resulting uncertainty block is 3×3. The corresponding uncertainty inputs and outputs were added to the synthesis model, using the recipe suggested in [8]. Each delta in (9) is a rank 1 perturbation in the A, B, C, and D matrices of the linear equations for the nominal flight condition. The δ_1 enters the first column of the nominal A matrix, corresponding to the β state, δ_2 enters the first column of the nominal B matrix, corresponding to the aileron input and δ_3 enters the second column of the nominal B matrix, corresponding to the rudder input. Uncertainties also enter one row of the C and D matrices, corresponding to the $\dot{\beta}$ output, but they are sufficiently small and we decided to ignore them. This assumption, also, simplifies the synthesis equations, since it makes D_{11} matrix of the synthesis model zero.

The H-infinity algorithm produced a state feedback gain matrix K which minimizes the infinity norm of the transfer matrix T_{zw} described above. The synthesis model and the resulting gain matrix F are available from authors upon request.

Throughout the rest of the paper the symbols $K_{.a}$ denote the state feedback gains in the aileron command computation and the symbols $K_{.r}$ denote the feedback gains in rudder command computation.

The heading hold mode is derived from the localizer capture and track mode by setting the gains K_y and $K_{\int y_e}$, obtained from the state feedback H-infinity solution, equal to zero in both rudder and aileron command computations:

$$\delta_{ac} = K_{\beta a}\beta + K_{Pa}P + K_{\phi a}\phi + K_{Ra}R + K_{\psi a}(\psi - \psi_c) + K_{\int \beta ea} \int \beta \tag{10}$$

$$\delta_{rc} = K_{\beta r}\beta + K_{Pr}P + K_{\phi r}\phi + K_{Rr}R + K_{\psi r}(\psi - \psi_c) + K_{\int \beta er} \int \beta. \tag{11}$$

There is no need to put an integrator on the heading error $\psi - \psi_c$, since there is already an integrator in the transfer functions from aileron and rudder to the heading angle ψ.

Gain Scheduling

The nominal controller performance was checked for all 14 flight conditions. For several of them the closed loop damping re-

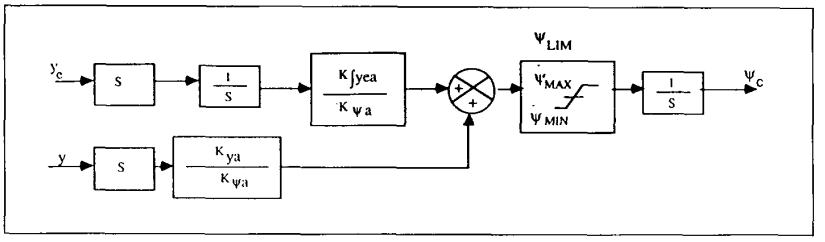

Fig. 6. Localizer capture and track mode.

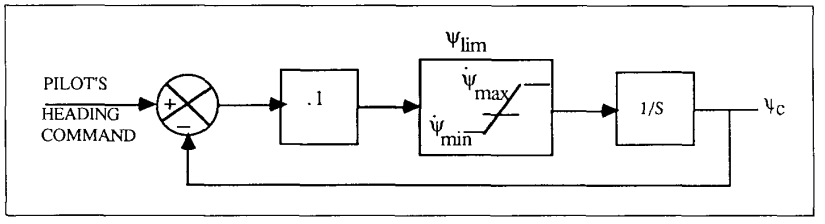

Fig. 7. Heading command filter.

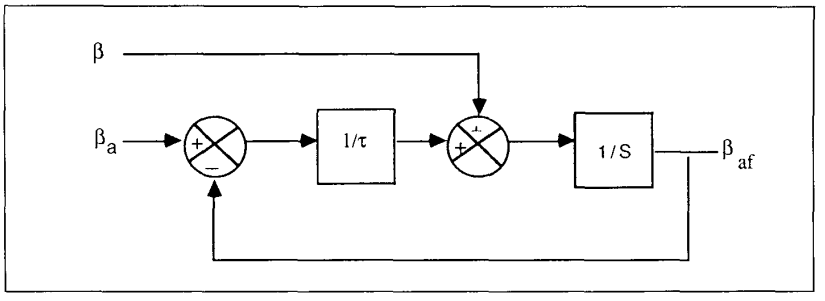

Fig. 8. β_{af} complementary filter.

der command computation were nulled to avoid having to introduce another limiter:

$$\delta_{rc} = K_{\beta r}\beta + K_{Pr}P + K_{\phi r}\phi + K_{Rr}R + K_{\psi r}\psi + K_{\int \beta er}\int \beta_e. \quad (17)$$

This change did not cause any significant degradation in either the stability or the performance of the feedback system.

The expressions (16), (17), (10), and (11) indicate an inner/outer loop structure of the localizer capture and track controller. The heading-hold controller can be thought of as an inner loop and the localizer capture and track controller as an outer loop. This structure is shown in Fig. 5.

As previously mentioned, the signal ψ_c in both heading and localizer modes must be rate limited to satisfy the maximum bank angle requirements ($\pm 30°$). The implementation of this limiter for the two modes are quite different and are described separately.

Bank Angle Limiting in Localizer Capture and Track Mode

The localizer capture and track mode was implemented using the so-called delta coordinates concept [12]. In this implementation (which in practice is done in discrete time), all the inputs to the controller (sensor signals and commands) are differentiated and all the outputs of the controller are integrated. The detailed diagram of the resulting implementation of the localizer mode is shown in Fig. 6.

As one can see from the diagram, the rate limiter becomes an amplitude limiter in the "delta coordinates." The value of the $\dot{\psi}$ limit was made a function of the crosstalk angle ($\psi_R - \psi$) at the localizer mode engagement. If $|\psi_R - \psi| > 45°$, then the airplane is flying towards the beam and is prevented from turning further into the beam by setting the corresponding bank angle limit to zero. For example, if the airplane is to the left of the beam at the localizer engagement, then it is only allowed negative banking:

$$\phi_{max} = 0 \qquad \dot{\psi}_{max} = 0 \quad (18)$$

$$\phi_{min} = -30 \qquad \dot{\psi}_{min} = g \tan(-30)/V_i.$$

Therefore, for high initial values of the crosstalk angle, the airplane will maintain its current heading, until it has to turn to align itself with the runway centerline. When the airplane is on the beam, the value of ϕ_{max} (respectively, ϕ_{min}) is relaxed to 30° (respectively, −30°). On the other hand, if at the time of localizer engagement, the airplane's groundtrack heading ψ_{gt} is equal to the runway heading angle, the airplane must be allowed both positive and negative banking, first to turn into the beam and then to align itself with the runway. In this case, the bank angle limit is ±30°:

$$\phi_{max} = 30 \qquad \dot{\psi}_{max} = g/\tan 30$$

$$\phi_{min} = -30 \qquad \dot{\psi}_{min} = g/\tan(-30). \quad (19)$$

Bank Angle Limiting in the Heading-Hold Mode

In the heading-hold mode, the pilot's heading command is processed by a first order filter and then sent to the heading controller, as shown in Fig. 7.

The necessary $\dot{\psi}$ limiting is done inside the filter as an amplitude limiter on $\dot{\psi}_c$. The selection of the filter's bandwidth (0.1 rad/s) was somewhat arbitrary, although we made sure that it was at most 1/3 of the heading controller bandwidth (which is at ~0.3 rad/s).

Effects of Crosswind

The problem specifications require that the airplane maintain a wings-level attitude when a crosswind is present. This requirement can be satisfied by driving the airmass sideslip angle (defined below) to zero and using the groundtrack heading angle instead of the heading angle as a feedback signal. It is common to model the effects of crosswind by defining a new input β_g [11]. Then β_{air} is defined to be the airmass sideslip angle:

$$\beta_{air} := \beta - \beta_g.$$

The groundtrack heading ψ_{gt} is defined by the following formula where α is the angle of attack and γ is the flight path angle:

$$\psi_{gt} = \psi + (\beta - \phi \sin\alpha)/\cos\gamma. \quad (20)$$

The lateral displacement y is rewritten in terms of ψ_{gt}:

$$y = (1/s)V_i \sin\psi_{gt}. \quad (21)$$

As previously noted, the airmass sideslip β_{air} must be driven to zero. The signal β_{air} is usually sensed by a β vane which is very noisy, and which is reliable only in the low

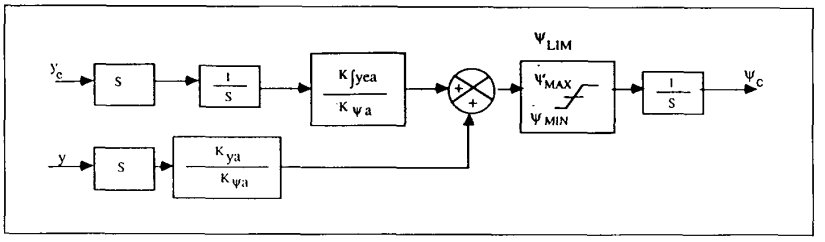

Fig. 6. Localizer capture and track mode.

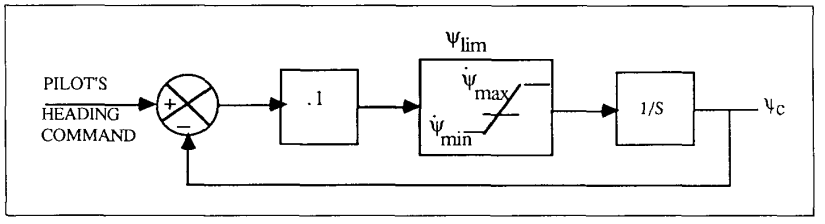

Fig. 7. Heading command filter.

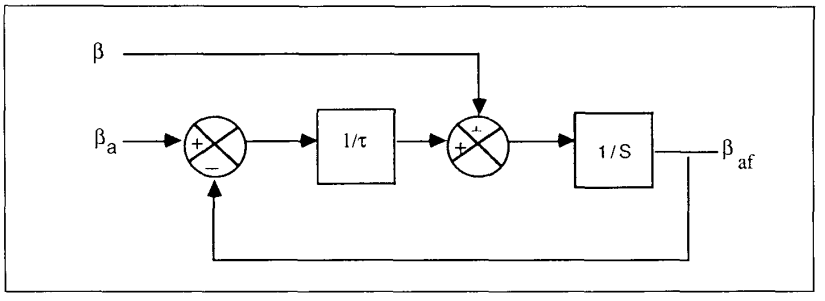

Fig. 8. β_{af} complementary filter.

der command computation were nulled to avoid having to introduce another limiter:

$$\delta_{rc} = K_{\beta r}\beta + K_{Pr}P + K_{\phi r}\phi + K_{Rr}R + K_{\psi r}\psi + K_{\int \beta er}\int \beta_e. \quad (17)$$

This change did not cause any significant degradation in either the stability or the performance of the feedback system.

The expressions (16), (17), (10), and (11) indicate an inner/outer loop structure of the localizer capture and track controller. The heading-hold controller can be thought of as an inner loop and the localizer capture and track controller as an outer loop. This structure is shown in Fig. 5.

As previously mentioned, the signal ψ_c in both heading and localizer modes must be rate limited to satisfy the maximum bank angle requirements ($\pm 30°$). The implementation of this limiter for the two modes are quite different and are described separately.

Bank Angle Limiting in Localizer Capture and Track Mode

The localizer capture and track mode was implemented using the so-called delta coordinates concept [12]. In this implementation (which in practice is done in discrete time), all the inputs to the controller (sensor signals and commands) are differentiated and all the outputs of the controller are integrated. The detailed diagram of the resulting implementation of the localizer mode is shown in Fig. 6.

As one can see from the diagram, the rate limiter becomes an amplitude limiter in the "delta coordinates." The value of the $\dot{\psi}$ limit was made a function of the crosstalk angle ($\psi_R - \psi$) at the localizer mode engagement. If $|\psi_R - \psi| > 45°$, then the airplane is flying towards the beam and is prevented from turning further into the beam by setting the corresponding bank angle limit to zero. For example, if the airplane is to the left of the beam at the localizer engagement, then it is only allowed negative banking:

$$\phi_{max} = 0 \qquad \dot{\psi}_{max} = 0 \quad (18)$$

$$\phi_{min} = -30 \qquad \dot{\psi}_{min} = g \tan(-30)/V_i.$$

Therefore, for high initial values of the crosstalk angle, the airplane will maintain its current heading, until it has to turn to align itself with the runway centerline. When the airplane is on the beam, the value of ϕ_{max} (respectively, ϕ_{min}) is relaxed to 30° (respectively, −30°). On the other hand, if at the time of localizer engagement, the airplane's groundtrack heading ψ_{gt} is equal to the runway heading angle, the airplane must be allowed both positive and negative banking, first to turn into the beam and then to align itself with the runway. In this case, the bank angle limit is ±30°:

$$\phi_{max} = 30 \qquad \dot{\psi}_{max} = g/\tan 30$$

$$\phi_{min} = -30 \qquad \dot{\psi}_{min} = g/\tan(-30). \quad (19)$$

Bank Angle Limiting in the Heading-Hold Mode

In the heading-hold mode, the pilot's heading command is processed by a first order filter and then sent to the heading controller, as shown in Fig. 7.

The necessary $\dot{\psi}$ limiting is done inside the filter as an amplitude limiter on $\dot{\psi}_c$. The selection of the filter's bandwidth (0.1 rad/s) was somewhat arbitrary, although we made sure that it was at most 1/3 of the heading controller bandwidth (which is at ~0.3 rad/s).

Effects of Crosswind

The problem specifications require that the airplane maintain a wings-level attitude when a crosswind is present. This requirement can be satisfied by driving the airmass sideslip angle (defined below) to zero and using the groundtrack heading angle instead of the heading angle as a feedback signal. It is common to model the effects of crosswind by defining a new input β_g [11]. Then β_{air} is defined to be the airmass sideslip angle:

$$\beta_{air} := \beta - \beta_g.$$

The groundtrack heading ψ_{gt} is defined by the following formula where α is the angle of attack and γ is the flight path angle:

$$\psi_{gt} = \psi + (\beta - \phi \sin\alpha)/\cos\gamma. \quad (20)$$

The lateral displacement y is rewritten in terms of ψ_{gt}:

$$y = (1/s)V_i \sin\psi_{gt}. \quad (21)$$

As previously noted, the airmass sideslip β_{air} must be driven to zero. The signal β_{air} is usually sensed by a β vane which is very noisy, and which is reliable only in the low

frequency range. Therefore, it was complemented with the inertial $\dot{\beta}$ signal at higher frequencies. Inertial $\dot{\beta}$ is not directly available, but it can be computed from other, available signals as follows, where N_y is the lateral body acceleration (g's) and θ is the pitch attitude:

$$\dot{\beta} = (g/V_i)N_y - (V_i/g)R\cos\alpha + (V_i/g)P \cdot \sin\alpha + \sin\phi\cos\theta$$

$$\beta = (1/s)\dot{\beta}. \tag{22}$$

The complementary filter to synthesize β_{air} is shown in Fig. 8.

The filter's time constant τ is to be determined from the sensor reliability information.

In the final design, to ensure proper response in the presence of crosswinds, the signals β and ψ were replaced by β_{af} and ψ_{gf}. Using ψ_{gf} instead of ψ as a feedback signal had little effect on stability for all flight conditions, and using β_{af} instead of β had no effect on stability.

Results

Linear and nonlinear analysis of the closed-loop system were performed to ensure compliance with the design requirements. Linear analysis was done for both localizer and heading controllers and consisted of the following items: 1) closed-loop eigenvalues; (2) Nyquist plots of all control and sensor loops; and 3) RMS responses to a 3 ft/s lateral Dryden gust.

The term "nonlinear analysis" is an exaggeration. Actually, a nonlinear controller (including $\dot{\psi}$ limiting) was connected to the linear model of the airplane and simulation was used to generate time histories for the localizer capture maneuver with the following set of initial conditions: the airplane is 5000 ft to the left of the beam with zero initial crosstrack angle. The maneuver was executed in 15 ft/s steady lateral crosswind.

Linear Analysis

Some of the linear analysis results are presented in Figs. 9 and 10. Fig. 9 shows the closed-loop eigenvalues for the localizer controller for all flight conditions. The damping ratios for all complex modes for both controllers satisfy the design requirements. The smallest damping ratio of the dominant mode is 0.6. The smallest damping ratio for the dutch roll mode is 0.45. Fig. 10 shows Nyquist plots for selected control and sensor loops. Simultaneous 4-dB 40° gain and phase margin requirement for each loop is equivalent to the condition that the Nyquist plot for that loop stays outside the

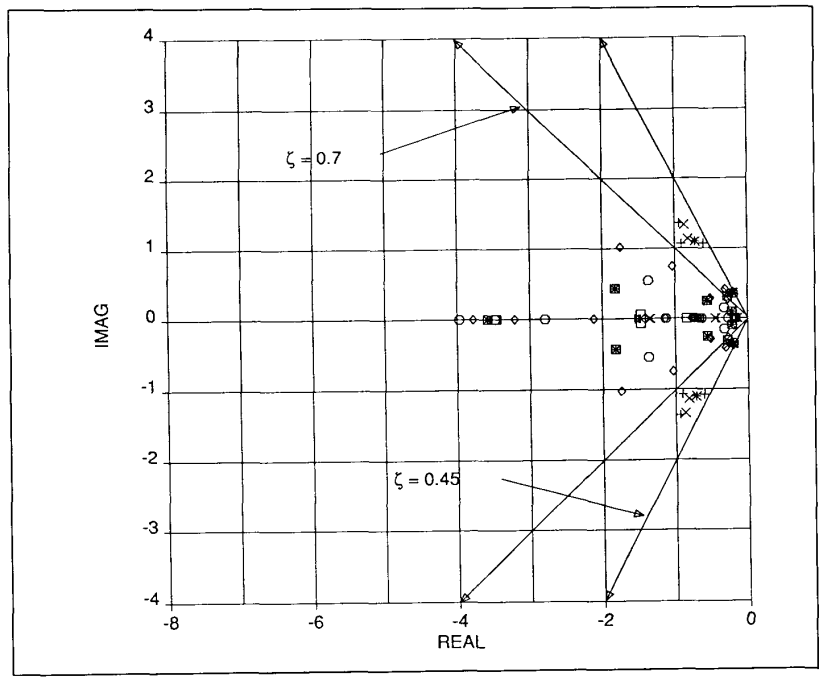

Fig. 9. Closed loop eigenvalues for all flight conditions of localizer capture and track mode.

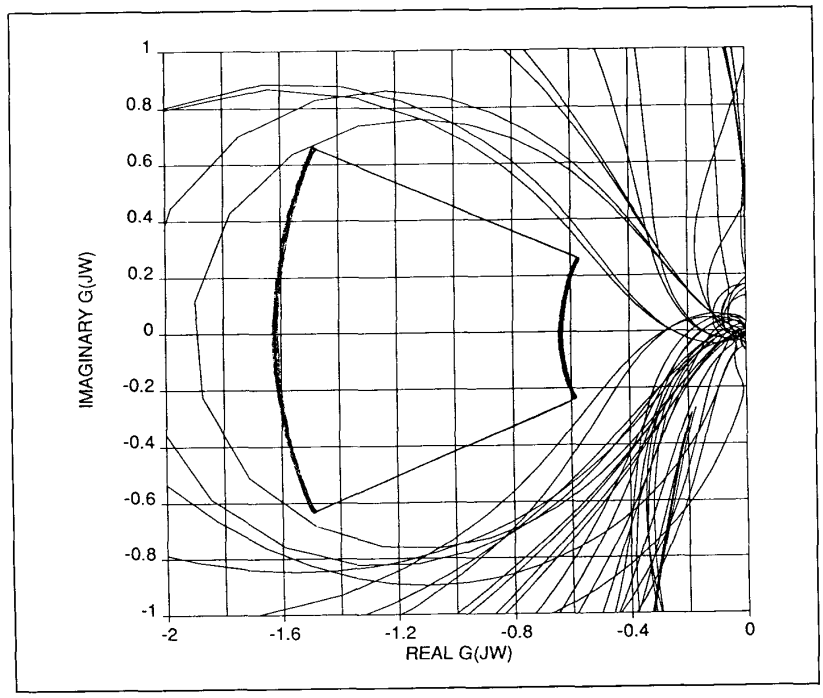

Fig. 10. Nyquist plots for selected flight conditions of localizer capture and track mode for all control and sensor loops.

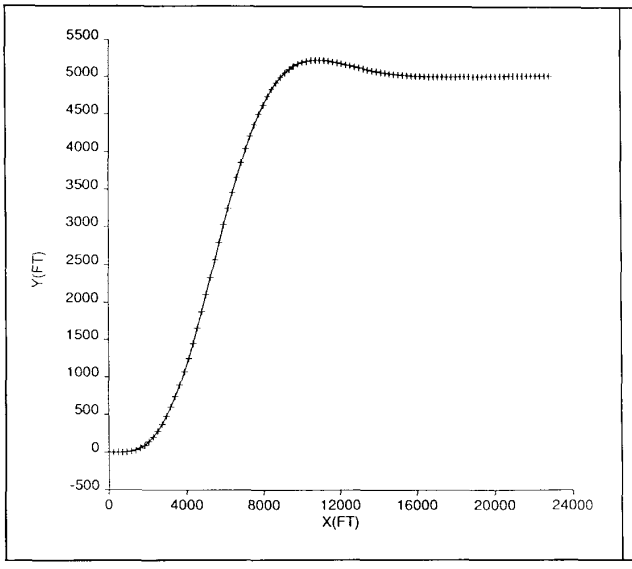

Fig. 11. Localizer capture and track mode in 15 ft/s crosswind (with initial offset from the beam of 5000 ft and initial crosstrack angle of 0°).

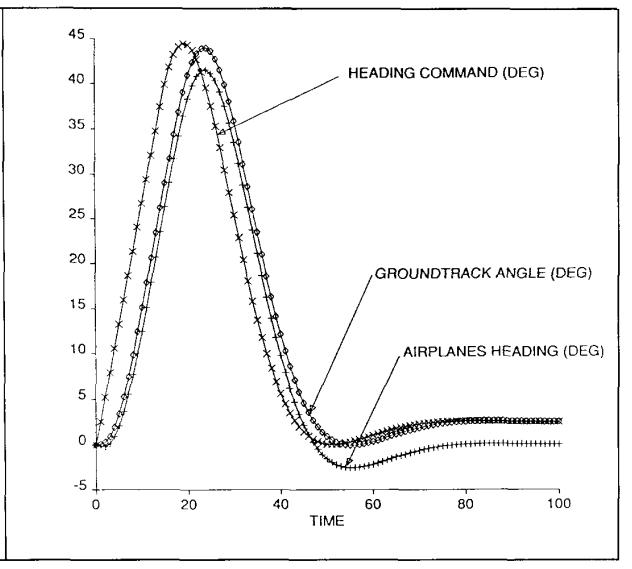

Fig. 12. Localizer capture and track mode in 15 ft/s crosswind (with initial offset from the beam of 5000 ft and initial crosstrack angle of 0°).

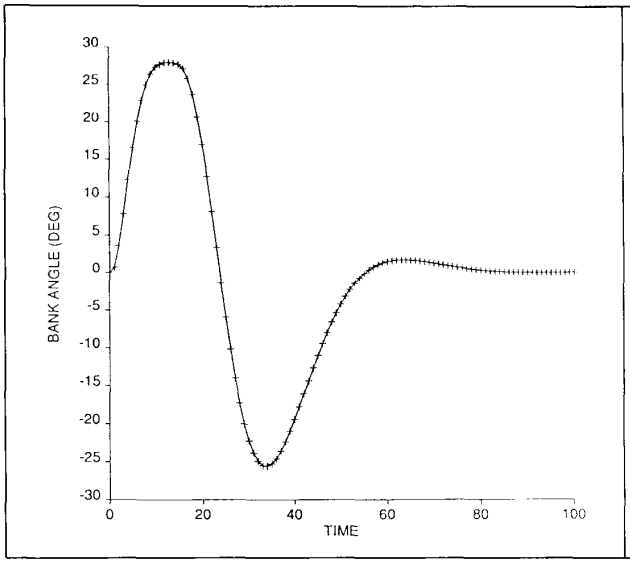

Fig. 13. Localizer capture and track mode in 15 ft/s crosswind (with initial offset from the beam of 5000 ft and initial crosstrack angle of 0°).

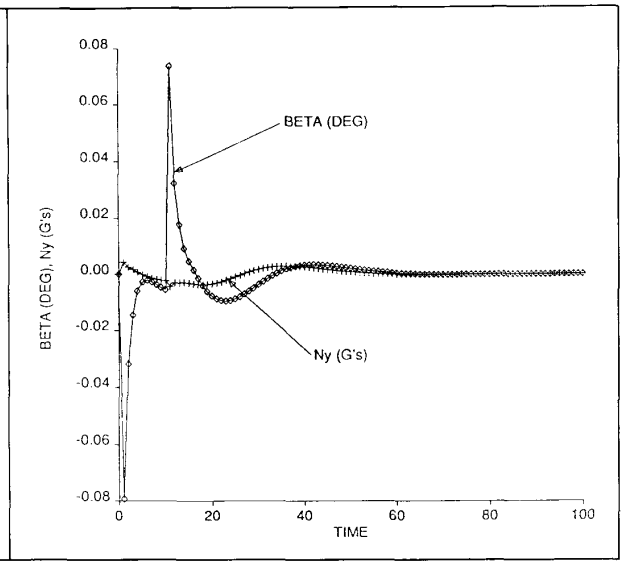

Fig. 14. Localizer capture and track mode in 15 ft/s crosswind (with initial offset from the beam of 5000 ft and initial crosstrack angle of 0°).

annular sector shown on the plot. This requirement is satisfied by all control and sensor loops. The rest of linear performance and robustness requirements have been satisfied by both localizer and heading controllers. Due to space limitations these results are not shown here. The details of the results are available from the authors upon request.

Nonlinear Analysis

The localizer capture maneuver with zero initial crosstrack angle in a 15 ft/s crosswind is shown in Figs. 11–14. The plot of the airplane's position in the x–y plane is shown in Fig. 11. The beam is 5000 ft to the right of the airplane, when a valid inertial landing system (ILS) signal is received. The airplane turns towards the beam and then captures it with negligible overshoot. Fig. 12 contains responses of the airplane's heading ψ, groundtrack heading ψ_{gt}, and heading command ψ_c, generated by the localizer mode (see Fig. 7). As one can see, the steady-state groundtrack heading is zero, whereas the airplane's heading angle is negative. The airplane feathered into the wind to maintain zero β_{air} and wings level, as indicated by the plot of the bank angle (Fig. 13). The bank angle limits at 30° during the turn towards the beam, and its steady-state value is zero, as required. Fig. 14 shows β_{air} and N_y. The steady-state airmass sideslip angle β_{air} is zero, thus making the airplane feather into

the wind. The lateral body acceleration N_y does not exceed 0.005 g, which is below the passenger discomfort threshold of 0.01 g.

Conclusions

After this design exercise, we feel that the recent developments in H-infinity synthesis theory have created a new and powerful tool for the synthesis of linear controllers. Since the algorithms are quite straightforward to apply and computationally efficient, we were able to focus most of our efforts on converting the given design requirements into the setting of the standard H-infinity synthesis problem. At present, this step is far from routine. However, it is unclear that this step could ever be automated, since design specifications are quite diverse and will rarely, if ever, come in the form of a standard mathematical synthesis problem. We did not use the μ-synthesis procedure in this paper. However, it turned out that with only a few iterations on the various weighting functions, we came up with a design which met all the specifications. We feel encouraged that the new tools for robust controller synthesis used here may lead to substantial savings in the overall effort required for the design of feedback control systems.

References

[1] J. C. Doyle, "Structured uncertainty in control system design," in *Proc. 24th IEEE Conf. Decision and Control*, Fort Lauderdale, FL, 1985, pp. 260–265.

[2] J. C. Doyle, K. Glover, P. P. Khargonekar, and B. A. Francis, "State-space solutions to standard H_2 and H_∞ control problems," *IEEE Trans. Auto. Control.*, vol. 34, no. 8, pp. 831–847, Aug. 1989.

[3] J. Doyle, K. Lenz, and A. Packard, "Design examples using μ-synthesis: Space shuttle lateral axis FCS during reentry," in *Proc. 25th IEEE Conf. Decision and Control*, Athens, Greece, 1986, pp. 2218–2223.

[4] K. Glover and J. C. Doyle, "State-space formulas for all stabilizing controllers that satisfy an H_∞ norm bound and relations to risk sensitivity," *Syst. Control Lett.*, vol. 11, pp. 167–172, 1988.

[5] P. P. Khargonekar, I. R. Petersen, and M. A. Rotea, "H_∞ optimal control with state feedback," *IEEE Trans. Auto. Control*, vol. AC-33, no. 8, pp. 786–788, 1988.

[6] P. P. Khargonekar, I. R. Petersen, and K. Zhou, "Robust stabilization of uncertain linear systems: Quadratic stabilizability and H-infinity control theory," *IEEE Trans. Auto. Control*, vol. 35, no. 3, pp. 356–361, Mar. 1990.

[7] A. J. Laub, "A Schur method for solving algebraic Riccati equations," *IEEE Trans. Auto. Control*, vol. AC-24, no. 6, pp. 913–921, 1979.

[8] B. G. Morton and R. M. McAfoos, "A μ-test for robustness analysis of a real-parameter variation problem," in *Proc. 1985 Amer. Control Conf.*, Boston, MA, 1985, pp. 135–138.

[9] I. R. Petersen, "Disturbance attenuation and H_∞ optimization: A design method based on the algebraic Riccati equation," *IEEE Trans. Auto. Control*, vol. AC-32, no. 5, pp. 427–429, 1987.

[10] G. Robel, "On computing the infinity norm," *IEEE Trans. Auto. Control*, vol. 34, no. 8, pp. 882–884, Aug. 1989.

[11] J. Roskam, *Airplane Flight Dynamics and Automatic Flight Controls*. Lawrence, KS: Roskam Aviation and Engineering Corp., 1982.

[12] P. Salo, "Delta coordinate controller implementation to avoid "fictitious gain" problem arising from gain scheduling," presented at Boeing Intercompany Controls Symp., Seattle, WA, 1987.

Isaac Kaminer received the B.S.E.E. and M.S.E. degrees from University of Minnesota in 1983 and 1985, respectively. From 1985 through 1989 he was with the Boeing Company, where he worked in the Guidance and Control Research Group for the last three years with the company. Currently he is pursuing the Ph.D. degree at the University of Michigan EECS Department. His research interests include robust control and numerical methods in control.

Pramod P. Khargonekar received the B.Tech. degree in electrical engineering from the Indian Institute of Technology, Bombay, in 1977, and the M.S. degree in mathematics, and the Ph.D. degree in electrical engineering from the University of Florida in 1980 and 1981, respectively. From 1981 to 1984, he was with the Department of Electrical Engineering, University of Florida, and from 1984 to 1989 he was with the Department of Electrical Engineering, University of Minnesota. In September 1989, he joined The University of Michigan where he is a Professor of Electrical Engineering and Computer Science. His research interests include robust and H_2/H_∞ optimal control, adaptive control, distributed systems, algebraic system theory, and applications to aerospace control problems. Dr. Khargonekar is the recepient of the Eckman award, the NSF Presidential Young Investigator award, and the George Taylor award. He was an associate editor of the *IEEE Transactions on Automtic Control* during 1987–1989. He is currently an associate editor of *Mathematics of Control, Signals, and Systems* and *Control Letters*.

Greg Robel was born in Yakima, WA, in 1955, and graduated with distinction from Harvey Mudd College in 1977, with a B.S. in mathematics. He received his Ph.D. degree in mathematics from The University of Michigan in 1982, where he specialized in the theory of operators on Hilbert space. From 1982 to 1986, he was an assistant professor of mathematics at Iowa State University. He joined The Boeing Company in 1986. His research interests include robust control and numerical methods in control. Dr. Robel is a member of the American Institute of Aeronautics and Astronautics, the American Mathemtical Society, the IEEE, and the Society for Industrial and Applied Mathemtics.